First Description of Arginine Catabolic Mobile Element (ACME) Type VI Harboring the *kdp* Operon Only in *Staphylococcus epidermidis* Using Short and Long Read Whole Genome Sequencing: Further Evidence of ACME Diversity

Brenda A. McManus, Aoife M. O'Connor, Sarah A. Egan, Peter R. Flanagan, David C. Coleman*

Microbiology Research Unit, Division of Oral Biosciences, Dublin Dental University Hospital, University of Dublin, Trinity College Dublin, Dublin 2, Republic of Ireland

Running title: Characterization of Novel ACME type VI

* Correspondence: David Coleman, Mailing address: Microbiology Research Unit, Division of Oral Biosciences, Dublin Dental University Hospital, University of Dublin, Trinity College Dublin, Dublin 2, Republic of Ireland. Phone: +353 1 6127276. Fax: +353 1 6127295. E mail: david.coleman@dental.tcd.ie.

Abbreviations: arginine catabolic mobile element; ACME, whole genome sequencing; WGS, direct repeat sequences; DRs, multilocus sequence typing; MLST, sequence types; STs, methicillin-resistant *Staphylococcus aureus*; MRSA, staphylococcal chromosomal cassette *mec*; SCC*mec*, coagulase negative staphylococci; CoNS

Abstract

The arginine catabolic mobile element (ACME) was first described in methicillin-resistant *Staphylococcus aureus* and is considered to enhance transmission, persistence and survival. Subsequently ACMEs were shown to be more prevalent in the coagulase-negative *Staphylococcus epidermidis*. Previously, ACME types were distinguished by characteristic combinations of the *arc* and *opp3* operons [I (*arc*+, *opp3*+), II (*arc*+, *opp3*-) and III (*arc*-, *opp3*+)] encoding an arginine deaminase pathway and oligopeptide permease transporter, respectively. Recently two novel ACME types harboring the potassium transporter-encoding operon *kdp* were described in oral *S. epidermidis* isolates [IV (*arc*+, *opp3*-, *kdp*+), and V (*arc*+, *opp3*+, *kdp*+)].

This study investigated two independent oral *S. epidermidis* isolates that yielded amplimers with *kdp*-directed primers only when subjected to ACME typing PCRs. Hybrid assemblies based on Illumina MiSeq short-read and Oxford Nanopore MinION long-read whole genome sequences revealed that both isolates harbored a sixth, novel ACME type (VI) integrated into *orfX*. Both ACME VIs lacked the *arc* and *opp3* operons, harbored the *kdp* operon adjacent to other commonly ACME-associated genes including *speG*, *hsd*, *sdr*, and *rep,* but the structural organization of the adjacent regions were distinct. These ACMEs were flanked by different direct repeat sequences and the ACME VI-positive isolates belonged to unrelated genetic clusters. Overall these findings are indicative of independent evolution. The identification of ACME type VI further illustrates the diversity of ACME elements in *S. epidermidis.* The presence of ACMEs harboring *kdp* may confer a selective advantage on oral *S. epidermidis* in a potassium-rich environment such as found in dental plaque.

Keywords: ACME; *Staphylococcus epidermidis*; *kdp* operon; potassium uptake; oral cavity.

1. Introduction

The arginine catabolic mobile element (ACME) was first described in the methicillin-resistant *Staphylococcus aureus* (MRSA) strain USA300 and since has been detected in other MRSA lineages and coagulase negative species including *Staphylococcus epidermidis*.

Similar to the staphylococcal chromosomal cassette element harboring *mec* (SCC*mec*), ACME is flanked by direct repeat sequences (DRs), integrates into *orfX* and is commonly collocated adjacent to SCC*mec* or SCC-associated genes in composite islands. Carriage of ACME is considered advantageous for isolate transmission, persistence and survival (Diep et al., 2006; Lindgren et al., 2014; O'Connor et al., 2018b; Planet et al., 2013). Furthermore, ACME is significantly more prevalent in *S. epidermidis* from diseased subgingival sites than in healthy subgingival sites (O'Connor et al., 2018b).

Until recently, ACMEs were differentiated into three main types based on distinct combinations of the *arc* (encoding an arginine deaminase pathway) and *opp3* (encoding an oligopeptide permease ABC transporter) operons. Types I (*arc*+, *opp3*+), II (*arc*+, *opp3*-) and III (*arc*-, *opp3*+) have been described in *S. epidermidis*, and types I, II and III (and variants thereof) have been detected in *S. aureus*. We recently described two novel ACME types harboring the *kdp* operon (encoding a potassium ABC transporter) in *S. epidermidis* defined as types IV (*arc*+, *kdp*+, *opp*-) and V (*arc*+, *kdp*+, *opp*+) (O'Connor et al., 2018a). Specific ACME types are commonly associated with particular *S. epidermidis* sequence types (STs) (McManus et al., 2017; O'Connor et al., 2018b, 2018a) indicating distinct evolutionary origins for each type. To date, ACMEs harboring *kdp* have been detected only in oral *S. epidermidis* isolates, suggesting that *kdp* may confer an advantage in this environment.

In this study we reveal the existence and genetic structure of a sixth distinct ACME type, designated VI (*arc*-, *kdp*+, *opp*-) harbored by two distinct lineages of oral *S. epidermidis* isolates by whole genome sequencing (WGS).

2. Materials and Methods

2.1 Isolates

Isolates were recovered by oral rinse sampling of two patients attending the Dublin Dental University Hospital and St. James's Hospital, Dublin. Sampling, isolate recovery, species and ACME type identification were carried out as previously described (O'Connor et al., 2018b).

2.2 Whole Genome Sequence Analysis

Genomic DNA was prepared as described previously (O'Connor et al., 2018b). Short-read sequencing libraries were prepared using Nextera XT library preparation reagents (Illumina, Eindhoven, The Netherlands) and sequenced using an Illumina MiSeq sequencer. Long-read sequencing was performed in multiplex with the MinION sequencing platform (Oxford Nanopore Technologies, Oxfordshire, UK) using the one-dimensional (1D) genomic DNA sequencing kit (SQK-LSK108) and ID native barcoding kit (EXP-NBD103) according to the manufacturer's instructions. Libraries were prepared using the NEBNext® Ultra™ II End Repair/dA-Tailing Module (New England Biolabs, Hertfordshire, UK) and barcodes were ligated using the NEB Blunt/TA Ligase Master Mix (New England Biolabs). Libraries were sequenced on an MK1B (MIN101B) MinION platform with a FLO-min 106 (SpotON R9.4) flow cell and using MinKNOW software version 1.7.10 (Oxford Nanopore Technologies).

Basecalls were performed on MinION Fast5 output files using Albacore v2.3.3 and demultiplexing was performed using Porechop v0.2.3. Hybrid genome assemblies for each isolate were generated by combining short- and long-reads using Unicycler v0.4.6 (Wick et al., 2017). Annotation was performed using BioNumerics version 7.6 (Applied Maths, Sint-Martens-Latem, Belgium) and BLAST (https://blast.ncbi.nlm.nih.gov/Blast.cgi). Genetic structures were visualized using the Artemis sequence viewer (Berriman and Rutherford, 2003) and Artemis Comparison Tool (Carver et al., 2005). Genetic structures of each ACME were confirmed by PCR for which primers were designed using ApE software version 2.0.51 and supplied by Merck (Wicklow, Republic of Ireland).

2.3 Multilocus Sequence Typing (MLST)

The sequence type (ST) of each isolate was determined using the *S. epidermidis* MLST plugin tool in Ridom SeqSphere+ v4.1.9 (Thomas et al., 2007).

2.4 Nucleotide sequence accession numbers

The nucleotide sequences of ACMEs characterized in oral *S. epidermidis* isolates 300OR1 and R02OR2 have been submitted to GenBank under accession numbers MK078515 and MK078516, respectively.

3. Results

Both isolates yielded amplimers with the *kdp*-directed PCR primers only. Analyses of the hybrid genome assemblies confirmed the presence of the complete *kdp* operon on an element integrated into *orfX*, flanked by DRs and the absence of the *arc* and *opp3* operons. The novel ACME

structure identified in both isolates was named ACME Type VI. The presence of *ccrC* recombinase genes was detected upstream of *kdp* in both isolates. (Fig. 1).

The ACME VI harbored by isolate 300OR1 was adjacent and directly downstream of a module harboring the *ccrAB2*-encoding recombinase genes and the *speG* gene encoding a spermidine acetyltransferase in a composite island (Fig. 1B). This ACME VI element was designated ACME subtype VIa and was demarcated by DR_C and DR_G. The DR_C has previously been identified at the 5′ terminus of all other ACME types (O'Connor et al., 2018b) and DR_G has been commonly identified internally in multiple ACME types (O'Connor et al., 2018b). Isolate 300OR1 belonged to ST327 (allelic profile 1-1-2-1-4-1-1).

The ACME VI element harbored by isolate R02OR2 was designated ACME subtype IVb and was demarcated by the novel DR, DR_Q (5′-GAAGCATATCACAAATAA-3′) and the previously described DR_I (O'Connor et al., 2018b) (Fig. 1C). Genes encoding heavy metal resistance were detected within the ACME VI composite island harbored by R02OR2. The *cop* and *ars* operons, commonly associated with ACME (O'Connor et al., 2018b), were detected in modules immediately downstream of ACME VIb and truncated at the 3′ by the novel DR_R (5′-GAAGGATATCATAAGTAA-3′). Genes encoding the transcriptional activator CadC and an immediately 3' adjacent cadmium resistance protein were detected within the ACME VIb module of this isolate (Fig. 1C). Isolate R02OR2 was identified as ST783 (allelic profile 8-19-17-4-62-10-2).

The *kdp* operon carried by ACME VI in both isolates exhibited 100% nucleotide sequence homology to each other and 99% nucleotide sequence identity to the *kdp* operon harbored by ACME types IV and V. Genes harbored by other ACME types such as *speG*, *hsd*, *sdr*, *rep* and lipopolysaccharide biosynthesis-encoding genes were detected in one or both of the ACME VI structures characterized and exhibited >93% nucleotide sequence homology.

4. Discussion

The two isolates investigated belonged to separate genetic clusters (GCs). A previous population structure analysis of *S. epidermidis* identified six GCs, one of which (GC6) is enriched with ACME-harboring isolates (Tolo et al., 2016). Based on the allelic profiles of these two isolates and their closest relatives (*S. epidermidis* MLST database accessed 5th October 2018), 300OR1 belongs to GC1, a GC associated with non-hospital sources and isolate R02OR2 belongs to the highly recombinant GC3 (Tolo et al., 2016). Importantly, other isolates belonging to these GCs

have not been subjected to ACME typing PCRs including *kdp*-targeting primers, and therefore the prevalence of ACMEs harboring the *kdp* operon in these GCs is currently unknown.

The diversity within the structural organization of the two ACME VI structures characterized and the distinct DRs flanking each element provides strong evidence that these elements evolved separately. However, the 100% nucleotide homology shared by the *kdp* operons within each element suggests that horizontal gene transfer may have played a role in the evolutionary pathway of ACME VI, at least to some extent. The detection of distinct ACME VI structures in isolates belonging to distinct GCs, may also indicate independent evolution.

Historically, ACME types have been distinguished by the distinct combinations of the *arc*, *opp3* and *kdp* operons present (Diep et al., 2006; Miragaia et al., 2009; O'Connor et al., 2018a). In the present study, due to the presence of only the *kdp* operon in ACME elements present in the two isolates investigated, both were classified as ACME VI. However, in accordance with previous studies of ACME diversity in *S. epidermidis* (O'Connor et al., 2018b), these ACME VI structures were distinguished into two distinct subtypes, VIa and VIb, based on distinct combinations of DRs demarcating each subtype (Fig. 1).

The proximal location of *kdp* to other genes commonly located within or adjacent to other ACME types further supports the conclusion that ACME VI is a distinct, novel ACME type rather than just a *kdp* operon acquired by horizontal gene transfer in isolation. Like the *kdp* operon of ACME type IV previously described in oral *S. epidermidis* isolates, the *kdp* operon was intact in ACME VI elements described in the present study. Similarly to oral *S. epidermidis* isolates harbouring ACME types IV and V (O'Connor et al., 2018a, 2018b), no native *kdp* genes were detected in the two *S. epidermidis* isolates harboring ACME VI. To date three of the six ACME types currently described and 14/37 ACME structures genetically characterized by WGS include the *kdp* operon (O'Connor et al., 2018b). As ACME is a large mobile genetic element ranging from to 27 - 117 kb that presumably incurs a fitness cost, we suggest that this operon provides an advantage to the host bacterium, particularly in a potassium-rich oral environment. It is likely that an additional ACME type harboring only the *kdp* and *opp3* operons will be detected in the future, further highlighting the extensive diversity of ACME.

176

177 **5. Declaration of Interest**

178 None

179 **6. Author Contributions**

180 BMcM conceived and designed the study, performed the WGS data analysis and drafted the
181 manuscript. AO'C, SE and PF assisted with the study co-ordination and WGS data analysis. DC
182 conceived the study, purchased the required materials, assisted with data analysis and drafted the
183 manuscript. All authors read and approved the final manuscript.

184 **7. Funding**

185 This research did not receive any specific grant from funding agencies in the public,
186 commercial, or not-for-profit sectors. This work was supported by the Microbiology Research
187 Unit, Dublin Dental University Hospital, Dublin, Ireland.

188 **8. Acknowledgments**

189 We thank Dr. Gráinne Brennan and Ms. Tanya Fleming at the National MRSA Reference
190 Laboratory at St. James's Hospital for their assistance with isolate identification. We are also
191 grateful to Keith Jolley for continuous curation of *S. epidermidis* MLST database.

192

193

194

195

196

197

198

199 **FIGURE LEGENDS**

200 FIGURE 1 Schematic diagram showing the genetic organization of previously described ACME
201 type IV (A) in *S. epidermidis* (GenBank accession number MG787421) and the comparative
202 organization of ACME subtypes VIa (B) and VIb (C) identified in two distinct oral *S.*
203 *epidermidis* isolates, defined according to the presence of the *kdp* operon, absence of the *arc* and
204 *opp3* operons and distinct combinations of flanking DRs. Arrows indicate the position and
205 orientation of open reading frames. Genes commonly associated with antimicrobial resistance,
206 SCC or ACME are shaded in color; *orfX* (black), *kdp* (purple), *speG* (dark grey), *copA* (lime
207 green), *pbp4* (dark green), and *ccr* (blue). Genes encoding the transcriptional activator CadC and
208 an immediately 3' adjacent cadmium resistance protein were detected in the ACME VI structure
209 harbored by R02OR2 only (mustard yellow).

210

211

212

213

214

215

216

217

218

219

220

221 **References**

222 Berriman, M., Rutherford, K., 2003. Viewing and annotating sequence data with Artemis. Br.
223 Bioinform 4, 124–132. https://doi.org/NO_DOI

224 Carver, T.J., Rutherford, K.M., Berriman, M., Rajandream, M.A., Barrell, B.G., Parkhill, J.,
225 2005. ACT: the Artemis Comparison Tool. Bioinformatics 21, 3422–3423.
226 https://doi.org/10.1093/bioinformatics/bti553

227 Diep, B.A., Gill, S.R., Chang, R.F., Phan, T.H. Van, Chen, J.H., Davidson, M.G., Lin, F., Lin, J.,
228 Carleton, H.A., Mongodin, E.F., Sensabaugh, G.F., Perdreau-Remington, F., 2006.
229 Complete genome sequence of USA300, an epidemic clone of community-acquired
230 meticillin-resistant *Staphylococcus aureus*. Lancet 367, 731–739.
231 https://doi.org/10.1016/S0140-6736(06)68231-7

232 Lindgren, J.K., Thomas, V.C., Olson, M.E., Chaudhari, S.S., Nuxoll, A.S., Schaeffer, C.R.,
233 Lindgren, K.E., Jones, J., Zimmerman, M.C., Dunman, P.M., Bayles, K.W., Fey, P.D.,
234 2014. Arginine deiminase in *Staphylococcus epidermidis* functions to augment biofilm
235 maturation through pH homeostasis. J Bacteriol 196, 2277–2289.
236 https://doi.org/10.1128/jb.00051-14

237 McManus, B.A., O'Connor, A.M., Kinnevey, P.M., O'Sullivan, M., Polyzois, I., Coleman, D.C.,
238 2017. First detailed genetic characterization of the structural organization of type III
239 arginine catabolic mobile elements harbored by *Staphylococcus epidermidis* by using
240 whole-genome sequencing. Antimicrob. Agents Chemother. 61, pii: e01216-17.
241 https://doi.org/10.1128/AAC.01216-17

242 Miragaia, M., de Lencastre, H., Perdreau-Remington, F., Chambers, H.F., Higashi, J., Sullam,
243 P.M., Lin, J., Wong, K.I., King, K.A., Otto, M., Sensabaugh, G.F., Diep, B.A., 2009.

Genetic diversity of arginine catabolic mobile element in *Staphylococcus epidermidis*. PLoS One 4. https://doi.org/10.1371/journal.pone.0007722

O'Connor, A.M., McManus, B.A., Coleman, D.C., 2018a. First description of novel arginine catabolic mobile elements (ACMEs) types IV and V harboring a *kdp* operon in *Staphylococcus epidermidis* characterized by whole genome sequencing. Infect. Genet. Evol. 61, 60–66. https://doi.org/10.1016/j.meegid.2018.03.012

O'Connor, A.M., McManus, B.A., Kinnevey, P.M., Brennan, G.I., Fleming, T.E., Cashin, P.J., O'Sullivan, M., Polyzois, I., Coleman, D.C., 2018b. Significant enrichment and diversity of the staphylococcal arginine catabolic mobile element ACME in *Staphylococcus epidermidis* isolates from subgingival peri-implantitis sites and periodontal pockets. Front. Microbiol. 9, 1558. https://doi.org/10.3389/fmicb.2018.01558

Planet, P.J., LaRussa, S.J., Dana, A., Smith, H., Xu, A., Ryan, C., Uhlemann, A.C., Boundy, S., Goldberg, J., Narechania, A., Kulkarni, R., Ratner, A.J., Geoghegan, J.A., Kolokotronis, S.O., Prince, A., 2013. Emergence of the epidemic methicillin-resistant *Staphylococcus aureus* strain USA300 coincides with horizontal transfer of the arginine catabolic mobile element and *speG*-mediated adaptations for survival on skin. MBio 4, e00889-13. https://doi.org/10.1128/mBio.00889-13

Thomas, J.C., Vargas, M.R., Miragaia, M., Peacock, S.J., Archer, G.L., Enright, M.C., 2007. Improved multilocus sequence typing scheme for *Staphylococcus epidermidis*. J Clin Microbiol 45, 616–619. https://doi.org/10.1128/jcm.01934-06

Tolo, I., Thomas, J.C., Fischer, R.S.B., Brown, E.L., Gray, B.M., Robinson, D.A., 2016. Do *Staphylococcus epidermidis* genetic clusters predict isolation sources? J. Clin. Microbiol. 54, 1711–1719. https://doi.org/10.1128/JCM.03345-15

Wick, R.R., Judd, L.M., Gorrie, C.L., Holt, K.E., 2017. Unicycler: Resolving bacterial genome

268 assemblies from short and long sequencing reads. PLoS Comput. Biol.
269 https://doi.org/10.1371/journal.pcbi.1005595

270

Figure 1

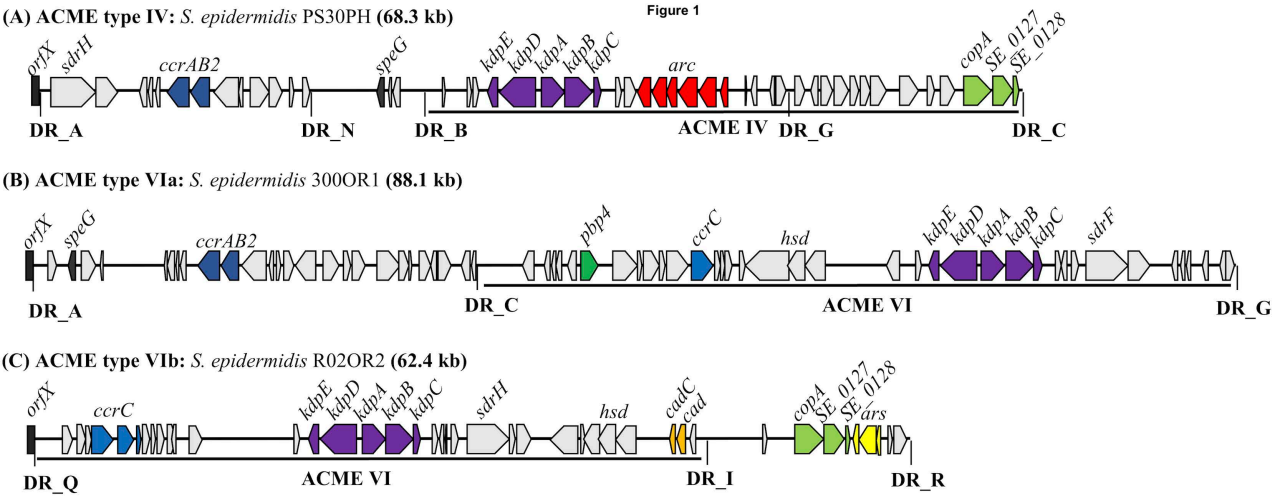
(A) ACME type IV: S. epidermidis PS30PH (68.3 kb)
orfX
sdrH
ccrAB2
speG
kdpE
kdpD
kdpA
kdpB
kdpC
arc
copA
SE_0127
SE_0128
DR_A
DR_N
DR_B
ACME IV
DR_G
DR_C
(B) ACME type VIa: S. epidermidis 300OR1 (88.1 kb)
orfX
speG
ccrAB2
pbp4
ccrC
hsd
kdpE
kdpD
kdpA
kdpB
kdpC
sdrF
DR_A
DR_C
ACME VI
DR_G
(C) ACME type VIb: S. epidermidis R02OR2 (62.4 kb)
orfX
ccrC
kdpE
kdpD
kdpA
kdpB
kdpC
sdrH
hsd
cadC
cad
copA
SE_0127
SE_0128
ars
DR_Q
ACME VI
DR_I
DR_R